Nitric Oxide xxx (xxxx) xxx–xxx

Contents lists available at ScienceDirect

Nitric Oxide

journal homepage: www.elsevier.com/locate/yniox

Subarachnoid hemorrhage induces neuronal nitric oxide synthase phosphorylation at Ser^{1412} in the dentate gyrus of the rat brain

Kentaro Wada[a], Koji Osuka[b,*], Yasuo Watanabe[c], Nobuteru Usuda[d], Motoaki Fukasawa[d], Yoshio Araki[a], Sho Okamoto[a], Toshihiko Wakabayashi[a]

[a] Department of Neurosurgery, Nagoya University Graduate School of Medicine, 65 Tsurumai Nagoya, Aichi, 466-8560, Japan
[b] Department of Neurological Surgery, Aichi Medical University, 1-1 Karimata Yazako, Nagakute, Aichi, 480-1195, Japan
[c] High Technology Research Center, Pharmacology, Showa Pharmaceutical University, 3-3165, Higashi-tamagawa Gakuen, Machida, Tokyo, 194-8543, Japan
[d] Department of Anatomy II, Fujita Health University School of Medicine, 1-98 Dengakugakubo, Kutsukake, Toyoake, Aichi, 470-1192, Japan

ARTICLE INFO

Keywords:
Cyclic AMP-dependent protein kinase
Dentate gyrus
Neuronal nitric oxide synthase
Subarachnoid hemorrhage

ABSTRACT

Introduction: We previously demonstrated that cyclic AMP-dependent protein kinase (PKA) phosphorylates neuronal nitric oxide synthase (nNOS) at Ser^{1412} in the hippocampal dentate gyrus after forebrain ischemia; this phosphorylation event activates NOS activity and might contribute to depression after cerebral ischemia. In this study, we revealed chronological and topographical changes in the phosphorylation of nNOS at Ser^{1412} immediately after subarachnoid hemorrhage (SAH).

Methods: In a rat single-hemorrhage model of SAH, the hippocampus and adjacent cortex were collected up to 24 h after SAH. Samples from rats that were not injected with autologous blood were used as controls. NOS was partially purified from crude samples via an ADP-agarose gel. Levels of nNOS, nNOS phosphorylated at Ser^{1412} (*p*-nNOS), PKA, and *p*-PKA at Thr^{197} were studied in the rat hippocampus and cortex using Western blot analyses and immunohistochemistry.

Results: According to the Western blot analysis, levels of *p*-nNOS at Ser^{1412} were significantly increased in the hippocampus, but not in the cortex, between 1 and 3 h after SAH. Immunohistochemistry revealed the phosphorylation of nNOS at Ser^{1412} and PKA at Thr^{197} in the dentate gyrus, but not in the CA1 area, 1 h after SAH. An injection of saline instead of blood also significantly increased levels of *p*-nNOS at Ser^{1412} in the hippocampus 1 h after the injection.

Conclusions: An immediate increase in intracranial pressure (ICP) might induce transient cerebral ischemia and promote the PKA-mediated phosphorylation of nNOS at Ser^{1412} in the dentate gyrus. This signal transduction pathway induces the excessive production of nitric oxide (NO) and might be involved in cognitive dysfunction after SAH.

1. Introduction

Various factors are associated with a poor outcome after subarachnoid hemorrhage (SAH). Previous studies have mainly focused on vasospasm and its sequela, which are involved in the high morbidity and mortality associated with SAH [1]. However, treatment with clazosentan, an endothelin receptor antagonist, after aneurysmal SAH has been shown to significantly reduce the incidence of vasospasm-related delayed ischemic neurological deficits (DINDs) and delayed cerebral infarctions but does not improve the poor neurological outcomes in patients with aneurysmal SAH [2]. Early brain injury (EBI) occurs immediately after SAH, is considered a physiological insult to the brain, and has recently been postulated to be the primary cause of the poor outcomes in patients with SAH [3]. A high proportion of survivors of SAH experience long-term cognitive impairment that affects their functional status and quality of life [4]. Cognitive dysfunction is increasingly recognized as a poor outcome after SAH [5]. However, its mechanism remains to be elucidated.

Increased proliferation of progenitor cells in the subgranular zone and neurogenesis in the dentate gyrus have often been observed in several experimental models of brain injury, including cerebral ischemia, hypoglycemia, seizure, and traumatic brain injury [6].

Abbreviations: PKA, cyclic AMP-dependent protein kinase; SAH, subarachnoid hemorrhage; ICP, intracranial pressure; EBI, early brain injury; CNS, central nervous system; CPP, cerebral perfusion pressure

* Corresponding author.
E-mail address: kosuka@aichi-med-u.ac.jp (K. Osuka).

http://dx.doi.org/10.1016/j.niox.2017.10.007
Received 22 June 2017; Received in revised form 7 October 2017; Accepted 22 October 2017

Minocycline enhances neurogenesis in the dentate gyrus and reduces the cognitive impairments in spatial learning and memory induced by experimental focal cerebral ischemia [7]. Nitric oxide (NO) acts as a neurotransmitter and is involved in learning, long-term potentiation and the regulation of cerebral blood flow in the central nervous system (CNS). Excess NO produced by neuronal nitric oxide synthase (nNOS) reacts with a superoxide anion to form the potent oxidant peroxynitrite, which causes primary brain injury [8]. Brain damage is substantially reduced in nNOS knockout mice after cerebral ischemia [9]. We previously reported that forebrain ischemia induces the phosphorylation of nNOS at Ser^{1412} in the dentate gyrus, which is suggested to negatively contribute to neurogenesis [10]. However, to date, the role of nNOS in the dentate gyrus after SAH has not been elucidated. Therefore, the present study was undertaken to determine whether phosphorylation of nNOS at Ser^{1412} occurs after SAH in rats. We also studied the distribution of nNOS phosphorylated at Ser^{1412} using an immunohistochemical technique to provide further information regarding regional differences in the reaction of nNOS in hippocampal neurons after SAH.

2. Methods

2.1. Materials

β-nicotinamide adenine dinucleotide phosphate (β-NADPH) was purchased from Oriental Yeast (Osaka, Japan). Unless specified otherwise, all other chemicals were obtained from Sigma-Aldrich Co., Ltd. (St. Louis, MO, USA).

2.2. Experimental model of SAH and saline injection

The experiments were performed in accordance with the National Institutes of Health Guidelines for the Care and Use of Laboratory Animals and with the approval of the Animal Care and Use Committee of Nagoya University Graduate School of Medicine. All efforts were made to minimize the number of animals used and their suffering. General anesthesia was induced in male Sprague-Dawley rats (300–350 g, Chubu Kagaku Shizai Ltd., Nagoya, Japan) using chloral hydrate (400 mg/kg, intraperitoneal (IP) injection). Then, the animals were intubated and ventilated with 1.0% halothane in an oxygen/nitrous oxide (30%/70%) gas mixture. The animals' temperature was monitored using a rectal probe and was maintained between 36.5 and 37.5 °C with a heating pad and lamp. The right femoral artery was exposed and catheterized using a 22-gauge catheter to enable blood sampling. A midline skin incision was created from the middle of the calvarium to the cervical spine during stereotactic surgery. The atlanto-occipital membrane was exposed under a microscope, and a 27-gauge needle was inserted into the cisterna magna. SAH was induced by infusing 300 μL of autologous arterial blood over a 1.5-min period. Additionally, the same dose of saline (300 μL) was injected instead of blood using the same procedure. The rats were maintained in a head-down position for 5 min to ensure that the blood or saline contacted the basilar artery; then, the needle was withdrawn and all wounds were sutured. Animals that did not receive an injection of blood or saline were used as controls.

2.3. Sample preparation for western blot analysis

One sample from each animal was prepared for analysis. Brain samples were obtained via decapitation under deep anesthesia at 1, 3, 6, 12 or 24 h after SAH (n = 6, each group) and 1 h after the saline injection (n = 5). Hippocampal and adjacent cortical samples at the same brain level were immediately dissected on ice, frozen in liquid nitrogen and stored at −80 °C until use. Brain samples from rats that were not subjected to SAH or the saline injections were used as controls (n = 6). Samples were homogenized in 15 vol of homogenization buffer containing 50 mmol/L Tris base/HCl (pH 7.5), 0.1 mmol/L dithiothreitol, 0.2 mmol/L EDTA, 0.2 mmol/L EGTA, 0.2 mmol/L phenylmethylsulfonyl fluoride (PMSF), 1.25 mg/mL pepstatin A, 0.2 mg/mL aprotinin, 5 nmol/L tetrahydrobiopterin (BH_4), 1 mmol/L sodium orthovanadate, 50 mmol/L sodium fluoride, 2 mmol/L sodium pyrophosphate, and 1% Nonidet P-40 (NP-40) using a homogenizer. Homogenates were then centrifuged at 15,000 g for 8 min at 4 °C. Protein concentrations of the supernatants were determined using the Bradford method and bovine serum albumin as the standard. Supernatant fractions were used as crude fractions. NOS was partially purified using 2′,5′-ADP-agarose, as previously described [11], to prepare the nNOS fractions. Briefly, 20 μL of 2′,5′-ADP-agarose and the same concentration of crude fraction (1500 μg/250 μL) were incubated with gentle mixing for 1 h at 4 °C. The agarose was washed with 200 μL of the homogenization buffer lacking NP-40, and nNOS was eluted from the 2′,5′-ADP-agarose using 50 μL of 10 mmol/L β-NADPH.

2.4. Western blot analysis

Extracts (12.5 μL) were separated on 7.5% SDS-PAGE gels, and proteins were transferred onto polyvinylidene difluoride (PVDF) membranes and incubated with a 1:200 dilution of a primary polyclonal antibody against nNOS phosphorylated (*p*) at Ser^{1412} (NP1412) and 1:750 dilution of an antibody against the catalytic subunits of cyclic AMP-dependent protein kinase (PKA C, Cell signaling Technology, Beverly, MA, USA) overnight at 4 °C. This NP1412 antibody only recognizes Ser^{1412}-phosphorylated nNOS [12]. Membranes were then incubated with a horseradish peroxidase-conjugated secondary antibody for 30 min at room temperature, and the antibody-bound proteins were visualized using enhanced chemiluminescence plus reagents (ECL plus; GE Healthcare, Buckinghamshire, UK). The NP1412 antibodies were stripped from the PVDF membranes and reblotted with a 1:3000 dilution of a primary monoclonal antibody against nNOS (Transduction Lab., Lexington, KY, USA) for 45 min at room temperature. Finally, membranes were developed using an ECL plus system, and band intensities were quantified by densitometric scanning using ImageQuant software (GE Healthcare).

In addition, Western blot analyses of the crude fractions were performed using 1:750 dilutions of antibodies against PKA C (Cell Signaling Technology) and PKA C phosphorylated at Thr^{197} (Cell Signaling Technology) by following the procedure described above.

2.5. Immunohistochemistry

Rats were perfused with 200 mL of ice-cold 4% paraformaldehyde in 0.1 mol/L sodium phosphate (pH 7.4) 1 h after SAH (n = 3). Brains were removed, placed in the fixation solution for 3 h and rinsed with 0.1 mol/L lysine hydrochloride in 0.1 mol/L phosphate-buffered saline for an additional 3 h. Serial coronal cryostat sections (10 μm) were stained using the avidin-biotinylated peroxidase complex (ABC) technique at room temperature. After blocking with 2% goat or horse serum for 30 min, sections were incubated with one of the following primary antibodies: rabbit anti-*p*-nNOS at Ser^{1412} (1:200), rabbit anti-nNOS (1:100, Sigma-Aldrich), rabbit anti-PKA C (1:500, Cell Signaling Technology) and rabbit anti-*p*-PKA C at Thr^{197} (1:500, Cell Signaling Technology). The incubation with a primary antibody was followed by successive incubations with biotinylated anti-rabbit IgG for 1 h and then ABC for 1 h. The sera used for the blocking step, the biotinylated antibodies, and ABC were purchased from Vector Laboratories (Burlingame, CA, USA). Reaction products were developed by incubating sections with 0.05% 3,3 -diaminobenzidine tetrachloride and 0.01% H_2O_2 in 50 mM Tris-HCl (pH 7.5) for 10 min. Rats that were not subjected to SAH were used as controls (n = 3).

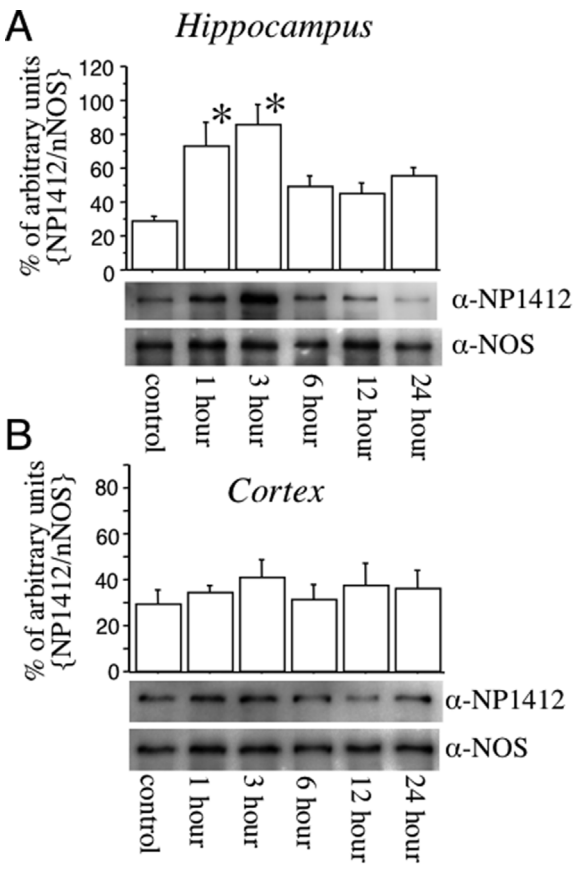

Fig. 1. Phosphorylation of nNOS at Ser^{1412} after SAH. At 1, 3, 6, 12 and 24 h after the intracisternal injection of autologous blood (300 μL), as indicated below the panel, nNOS was affinity-purified from the hippocampus (A) and cortex (B) by ADP-agarose affinity chromatography. These samples were subjected to Western blots using the anti-nNOS (α-nNOS) and anti-phosphorylated nNOS at Ser^{1412} (α-NP1412) antibodies. The histogram shows the amount of α-NP1412 relative to α-nNOS in the membrane. The means ± SEM of six animals are shown. Control; control basilar artery not subjected to SAH. *P < 0.05 indicates a significant difference between the control and SAH groups based on an ANOVA followed by Fisher's PLSD.

2.6. Statistical analysis

Data are expressed as mean values ± standard errors of the means (SEM). Significant differences between groups were assessed using one-way analysis of variance (ANOVA), followed by Fisher's protected least significant differences (PLSD) test for multiple comparisons. A P-value < 0.05 was considered significant.

3. Results

3.1. Effects of SAH on nNOS phosphorylation at Ser^{1412}

We first investigated whether SAH induced nNOS phosphorylation at Ser^{1412} (NP1412) in both the hippocampus and cortex of rat SAH models using a Western blot analysis. Compared with that in the control samples, an approximately 3-fold increase in nNOS phosphorylation at Ser^{1412} was observed in the hippocampus 1 h and 3 h after SAH (Fig. 1A). We did not detect significant changes in the levels of phosphorylated nNOS in the cortex (Fig. 1B). Equal levels of nNOS were purified from crude fractions, even after SAH, indicating that the SAH episode primarily modulated nNOS phosphorylation at Ser^{1412} in the hippocampus. The densitometric analysis of the NP1412/nNOS bands showed a significant increase compared with control values from 1 h to 3 h after SAH by one-way ANOVA and subsequent Fisher's PLSD test ($P < 0.05$).

3.2. Phosphorylation of nNOS at Ser^{1412} occurred in the dentate gyrus of the hippocampus

We then investigated in which region of the hippocampus nNOS phosphorylation at Ser^{1412} occurred; we meticulously explored levels of *p*-nNOS at Ser^{1412} in the hippocampus 1 h after SAH. Nonpyramidal neurons in the dentate gyrus were immunopositive for nNOS at Ser^{1412} 1 h after SAH (Fig. 2A, B and D *arrows*), whereas no apparent staining for *p*-nNOS at Ser^{1412} was observed in the CA1 area (Fig. 2A, C and E) or the CA3 area. These impressive findings led us to subsequently focus on the serial changes in the hippocampal dentate gyrus after SAH.

Then, we compared the expression levels of nNOS and *p*-nNOS at Ser^{1412} in the dentate gyrus of the hippocampus between the control and SAH rats. The nNOS immunoreactivity was primarily detected in neurons and was not detectably altered 1 h after SAH compared with that in the control rats (Fig. 3A and B). Intense immunoreactivity for *p*-nNOS at Ser^{1412} was observed in nonpyramidal neurons located in the dentate gyrus 1 h after SAH (Fig. 3D and F) but was not detected in the dentate gyrus of the control rats (Fig. 3C and E).

3.3. PKA C phosphorylation at Thr^{197} occurred in the hippocampus

Ser^{1412} of nNOS was previously identified as a potential PKA phosphorylation site *in vitro* [12]. We examined the temporal relationship between nNOS and PKA C phosphorylation after SAH. First, we investigated whether SAH induced PKA C phosphorylation at Thr^{197} in the hippocampus using the NP-40-soluble crude fractions. Approximately equal levels of β-actin and PKA C were detected in the crude fractions, even after SAH (Fig. 4). According to the densitometric analysis and one-way ANOVA followed by Fisher's PLSD, SAH significantly induced PKA C phosphorylation at Thr^{197} from 1 to 3 h after SAH ($P < 0.05$, Fig. 4), which is the same period in which nNOS is phosphorylated at Ser^{1412} in the hippocampus (Fig. 1A).

3.4. Neurons expressed PKA C phosphorylated at Thr^{197} in the dentate gyrus after SAH

Then, we examined the spatial relationship between nNOS and PKA C phosphorylation after SAH. PKA C was mainly observed in the cytoplasm of nonpyramidal neurons in the dentate gyrus both in the control rats and 1 h after SAH (Fig. 5A and B). The immunoreactivity of *p*-PKA C at Thr^{197} was observed in the neurons in the subgranular layer of the dentate gyrus 1 h after SAH (Fig. 5D and F), which is the same location observed for nNOS phosphorylated at Ser^{1412} (Fig. 3D and F), but *p*-PKA C at Thr^{197} immunoreactivity was not observed in the dentate gyrus in the control rats (Fig. 5C and E).

3.5. Colocalization of nNOS and PKA C after SAH

We explored the interaction between PKA C and nNOS in the hippocampus using ADP-agarose affinity chromatography. PKA C was present in the NOS fraction after SAH, suggesting that PKA colocalized with nNOS after SAH (Fig. 6).

3.6. Effects of saline on nNOS phosphorylation at Ser^{1412}

We injected the same volume of saline or autologous blood into the cisterna magna and removed the hippocampus 1 h after SAH to further investigate the mechanism by which SAH induced nNOS phosphorylation at Ser^{1412}. As shown in the immunoblot analyses and subsequent one-way ANOVA followed by Fisher's PLSD, nNOS phosphorylation at Ser^{1412} was significantly increased by approximately 3.5-fold following the saline injection compared with the control level ($P < 0.05$, Fig. 7). This increase was nearly equivalent to the increase observed following the autologous blood injection.

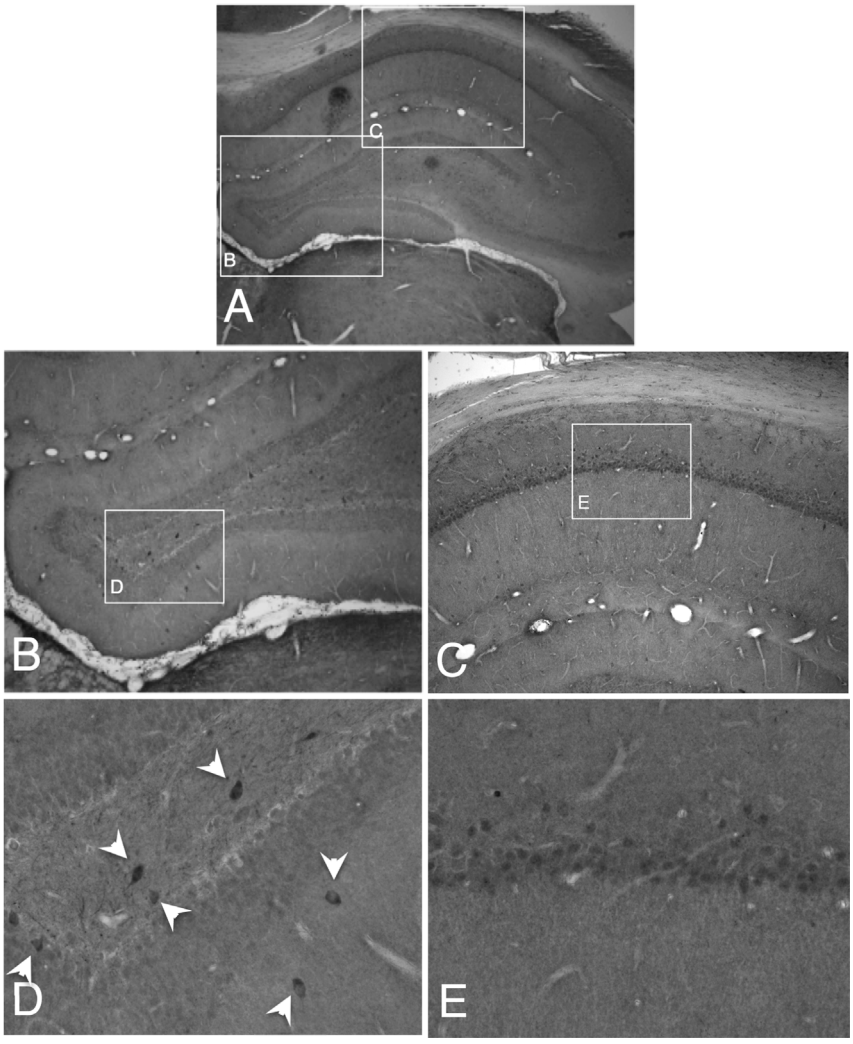

Fig. 2. Immunohistochemical staining for nNOS phosphorylated at Ser^{1412} (NP1412) in the hippocampus after SAH. Rats were perfused with 4% paraformaldehyde 1 h after an injection of autologous blood. Ten-micrometer coronal slices were immunostained with an antibody recognizing NP1412 using the ABC method. The whole image of the left hippocampus is shown (A). The dentate gyrus areas in the white rectangle, which are labeled in A and B, are shown at a higher magnifications in B and D, respectively. The CA1 areas in the white rectangle, which are labeled in A and C, are shown at a higher magnifications in C and E, respectively. Note that positive staining for the NP1412 antibody was observed in the nonpyramidal neurons in the dentate gyrus 1 h after SAH (D, arrows), but no apparent staining was observed in CA1 (C and E).

4. Discussion

This study is the first to clarify that SAH immediately and significantly induced nNOS phosphorylation at Ser^{1412} in the hippocampal dentate gyrus concomitant with PKA phosphorylation. The increased intracranial pressure (ICP) after SAH might induce nNOS phosphorylation at Ser^{1412}.

We have often used endovascular perforation and blood injections into the cisterna magna to study the mechanism underlying cerebral vasospasm after SAH in rats [13–15]. The advantage of injecting blood into the cisterna magna is that the injections are easy to perform and have a lower mortality rate than the endovascular perforation model [14,15]. The single intracisternal injection of 300 μL of autologous blood or saline immediately increases the ICP to approximately 50 mmHg [14]. If we inject autologous blood (300 μL) at a higher injection velocity over 15 s, the ICP substantially increases up to 100 mmHg. Using the same conditions, the ICP also increased up to 70 mmHg after an injection of 300 μL saline [16]. The dose and injection rate of the autologous blood or saline might determine the degree of the increase in the ICP. An intracisternal injection of autologous blood decreases the cerebral perfusion pressure (CPP) and induces cerebral ischemia under the circumstances of an elevated ICP [17]. A clinically high ICP is a common complication that occurs immediately after SAH in severe cases and is associated with EBI [18]. Neuronal apoptosis in the dentate gyrus was confirmed in patients with cerebral ischemia and in patients with SAH [19]. In terms of neuronal cell death, the severity of EBI linearly correlates with the reduced CPP during hyperacute SAH [20]. Approximately two-thirds of patients suffer from cerebral ischemia at 1–3 days after the onset of SAH, which was clinically revealed in a magnetic resonance imaging (MRI) study [21]. In particular, 81% of poor-grade patients display ischemic findings on diffusion-weighted images within 24 h after SAH [22]. An injection of subarachnoid blood hemolysate produced DNA fragmentation and apoptotic cell death in the mouse cortex, but an injection of saline did not produce these results [23]. However, the administration of the same volume of both autologous blood and saline significantly increased the level of *p*-nNOS at Ser^{1412} compared with that in the control rats. Therefore, early cerebral ischemia, which was induced by the increased ICP, might be the cause of EBI rather than extravasated blood hemolysate after SAH.

PKA plays a critical role in the various intracellular metabolic and physiological effects of cAMP. The late phase of long-term potentiation and memory were triggered by PKA in mice [24]. After forebrain or global ischemia, calcium/calmodulin-dependent protein kinase II (CaM-KII) activity in the hippocampus was rapidly and extensively decreased, whereas the PKA activity was not significantly changed [25,26]. Based on the known regional-specific vulnerability of the hippocampal tissue to ischemic insult, a significant reduction in PKA activity in the CA1 subfield was revealed during the acute phase of cerebral ischemia, without significant changes in the CA3 subfield or dentate gyrus [27]. PKA is activated after forebrain ischemia [10]. Based on our immunohistochemical staining, the catalytic subunits of PKA (PKA C) are located in the cytoplasm of neurons in the dentate gyrus. One hour after SAH, PKA C phosphorylated at Thr^{197} is located in

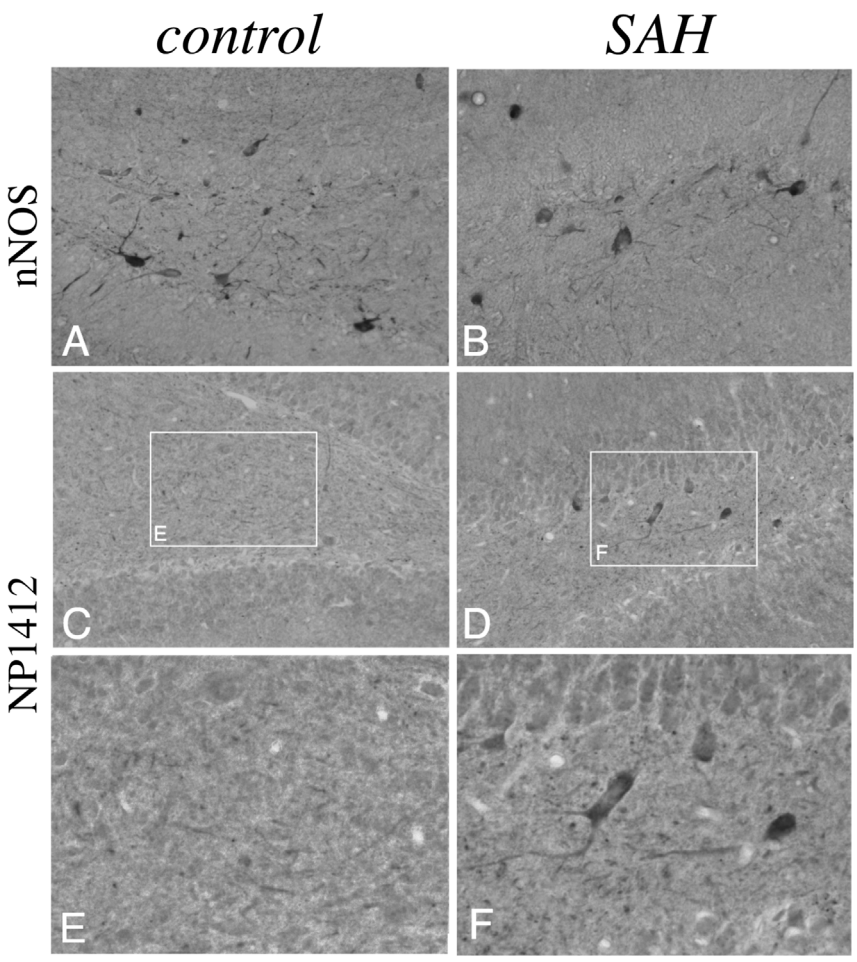

Fig. 3. Immunohistochemical analysis of the levels of nNOS and nNOS phosphorylated at Ser^{1412} (NP1412) in the hippocampal dentate gyrus area after SAH. One hour after the sham operation (A, C and E) or SAH (B, D and F), rats were perfused with 4% paraformaldehyde. Ten-micrometer coronal slices were immunostained with antibodies recognizing either nNOS (A and B) or NP1412 (C, D, E and F) using the ABC method. The dentate gyrus areas in the white rectangle, which are labeled in C and D, are shown at a higher magnifications in E and F, respectively. The nNOS immunoreactivity was preserved 1 h after SAH (B) compared with that in the sham animals (A). Positive staining for the NP1412 antibody was observed in nonpyramidal neurons in the dentate gyrus 1 h after SAH (D and F) compared with that in the sham group (C and E).

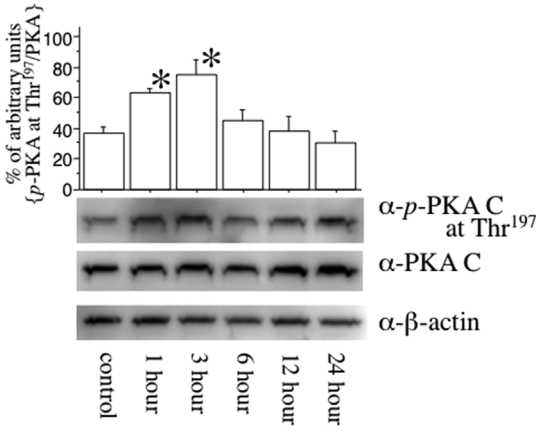

Fig. 4. Phosphorylation of PKA C at Thr^{197} in the hippocampus after SAH. At 1, 3, 6, 12 and 24 h after the intracisternal injection of the autologous blood (300 μL), as indicated below the panel, the NP-40-soluble fractions (crude fractions) were subjected to Western blots using the anti-PKA C (α-PKA C), anti-phosphorylated PKA C at Thr^{197} (α-*p*-PKA C at Thr^{197}) and anti-β-actin antibodies. The histogram shows the amount of α-*p*-PKA C at Thr^{197} relative to α-PKA C in the membrane. The means ± SEM of five animals are shown. Control; control basilar artery not subjected to SAH. *P < 0.05 indicates a significant difference between the control and SAH groups based on an ANOVA followed by Fisher's PLSD.

the nuclei of these neurons, suggesting that PKA signaling is also activated and plays a role as a messenger in the dentate gyrus after both cerebral ischemia and SAH.

PKA phosphorylates nNOS in the CNS [28–30]. PKA and CaM-KII stoichiometrically phosphorylate NOS at different serine residues. Phosphorylation of nNOS at Ser^{847} and Ser^{741} is directly mediated by CaM-KII and CaM-KI, respectively, leading to a reduction in NOS activity [31–33]. Phosphorylation of nNOS at Ser^{1412} has been shown to induce NO production under physiological conditions. nNOS initiates penile erection through the generation of NO, and the PKA-mediated phosphorylation of nNOS at Ser^{1412} has been shown to mediate penile erectile physiology, including sustaining penile erection [34]. AMP-activated protein kinase (AMPK) phosphorylates nNOS at Ser^{1412} after cerebral ischemia and reperfusion injury, which is associated with increased nNOS activity [35]. Moreover, nNOS plays a critical role in regulating cardiomyocyte function. Oxidative stress induces nNOS phosphorylation at Ser^{1412} in cardiomyocytes via AMPK, concomitant with the increased NO production [36]. Protein kinase D also phosphorylates nNOS at Ser^{1412} *in vitro* and *in vivo* in living cells, thereby increasing nNOS enzymatic activity and resulting in NO production [37]. In this study, SAH significantly increased levels of phosphorylated PKA 1–3 h after SAH, which is the same time course as the increase in levels of nNOS phosphorylated at Ser^{1412}. Furthermore, the phosphorylation of both nNOS and PKA occurred in the dentate gyrus. Based on our data, PKA might be closely associated with nNOS activity in the hippocampal dentate gyrus after SAH. However, PKA, Akt and CaM-KII phosphorylate nNOS at Ser^{1412} *in vitro* [12]. These other protein kinases may phosphorylate nNOS at Ser^{1412} after SAH.

Neurons are continuously generated in the hippocampal dentate gyrus of adult macaque monkeys and humans throughout life [38,39]. The expression of nNOS is tightly correlated with neurogenesis in the subgranular zone of the dentate gyrus [40]. NO has been shown to have important roles in adult neurogenesis [41]. However, neurogenesis depends on the specific isoform of NOS. Neurogenesis is stimulated by NO from inducible NOS in the dentate gyrus after focal cerebral

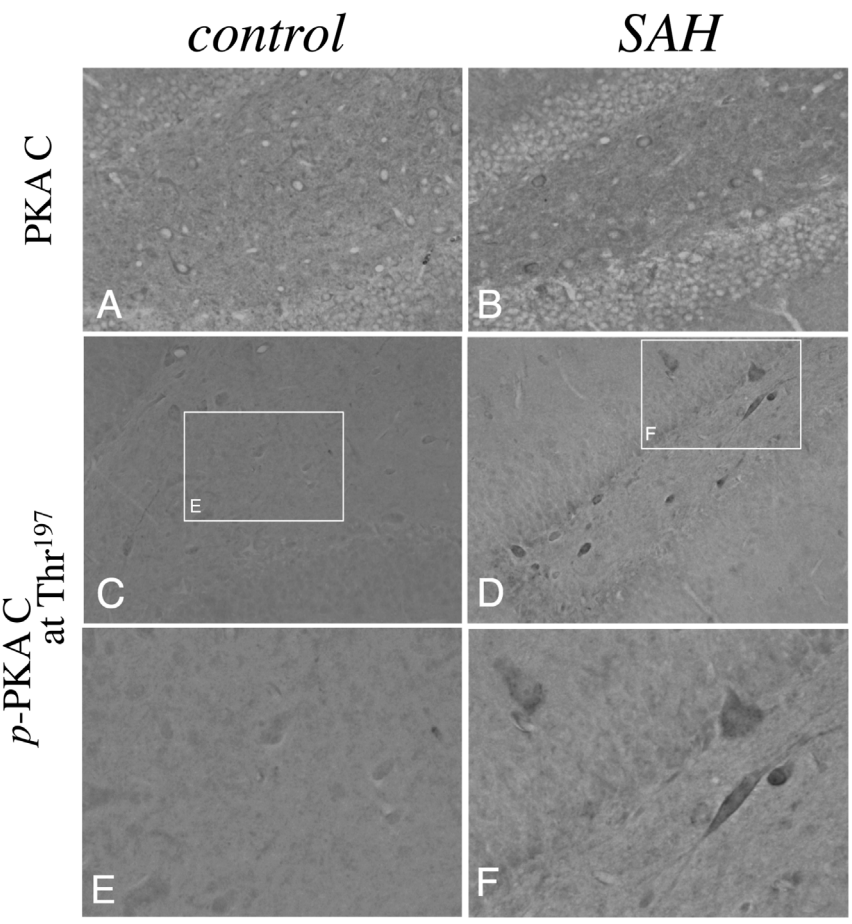

Fig. 5. Immunohistochemical analysis of levels of PKA C and PKA C phosphorylated at Thr^{197} (*p*-PKA C at Thr^{197}) in the hippocampal dentate gyrus area after SAH. One hour after the sham operation (A, C and E) or SAH (B, D and F), rats were perfused with 4% paraformaldehyde. Ten-micrometer coronal slices were immunostained with antibodies recognizing either PKA C (A and B) or *p*-PKA C at Thr^{197} (C, D, E and F) using the ABC method. The areas in the rectangle, which are labeled in C and D, are shown at higher magnifications in E and F, respectively. PKA C immunoreactivity was observed in the cytoplasm of nonpyramidal neurons in the dentate gyrus 1 h after SAH (B) compared with the sham animals (A). Positive staining for *p*-PKA C at Thr^{197} was evident, particularly in the nonpyramidal neurons located in the subgranular layer of the dentate gyrus, 1 h after SAH (D and F) compared with the sham animals (C and E).

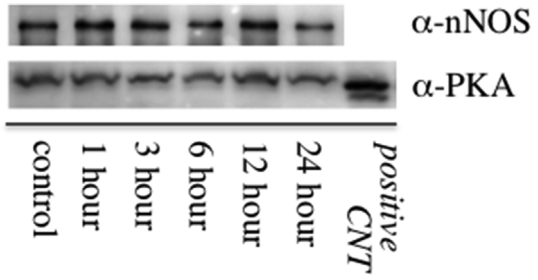

Fig. 6. Representative immunoblot analysis of nNOS and the PKA C levels in the hippocampus after subarachnoid hemorrhage. The NOS-containing fraction was prepared by ADP-agarose affinity chromatography and subjected to Western blot analysis with anti-nNOS (α-nNOS) and anti-PKA C (α-PKA C) antibodies. The data are representative of experiments from three series with the same results. Untreated Jurkat cells were lysed in Chaps cell extract buffer, and a cytoplasmic fraction (Cell Signaling Technology) served as the positive control for comparison.

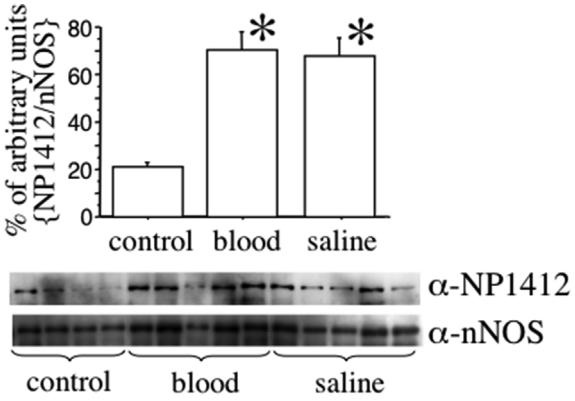

Fig. 7. The phosphorylation of nNOS at Ser^{1412} after an intracisternal injection of autologous blood (300 μL) or saline (300 μL). At 1 h after the intracisternal injection, as indicated below the panel, nNOS was affinity-purified from the hippocampus by ADP-agarose affinity chromatography and then subjected to Western blots using anti-nNOS (α-nNOS) and anti-phosphorylated nNOS at Ser^{1412} (α-NP1412) antibodies. The histogram shows the amount of α-NP1412 relative to α-nNOS in the membrane. The means ± SEM of four or five animals are shown. Control; control basilar artery not subjected to injection. *P < 0.05 indicates a significant difference compared with the control based on an ANOVA followed by Fisher's PLSD.

ischemia [42,43]. The experimental model will determine the effect of NO produced by neuronal NOS on the dentate gyrus. The chronic inhibition of nNOS with an inhibitor increases cell proliferation and has no effect on cell death in the dentate gyrus in the rat hippocampus in the absence of cerebral injury [44]. Under transient focal cerebral ischemia conditions, NO produced by nNOS is an inhibitory regulator of neurogenesis in the ischemic subgranular layer of the dentate gyrus [45]. Cerebral ischemia results in a significant decrease in neurogenesis in the dentate gyrus compared with that in controls 3 days after the onset of SAH [46]. The excess NO produced by nNOS phosphorylated at Ser^{1412} immediately after SAH reacts with the superoxide anion to form the potent harmful peroxynitrite [8], potentially causing neuronal cell damage in the dentate gyrus. The phosphorylation of nNOS at Ser^{847} by CaM-KII in the CA1 region of the hippocampus after SAH attenuates nNOS activity and contributes to the resistance to damage in neurons [47]. Altogether, these findings suggest the presence of a regionally distinct system for regulating nNOS activity in the CA1 and dentate gyrus immediately after SAH.

Stress exerts a profound effect on neurogenesis, leading to a prolonged decrease in the rate of cell proliferation in the adult hippocampus [48]. Antidepressant interventions are capable of inducing

neurogenesis in the nonhuman primate hippocampal dentate gyrus [49,50]. Over-expression of nNOS plays critical roles in the pathogenesis of chronic stress-induced depression in mice [51]. The dentate gyrus plays a stronger role in declarative memory acquisition and pattern separation than CA1 pyramidal cells [52,53]. Based on the data from the present investigation and previous studies, the phosphorylation of nNOS at Ser^{1412} in the dentate gyrus after SAH might negatively regulate neurogenesis and be involved in cognitive dysfunction after SAH. The inhibition of this signaling pathway in the hippocampus represents a potentially novel approach to the prevention of neuropsychological disorders after SAH.

5. Conclusions

The present investigation was the first to clarify that the phosphorylation of PKA in the dentate gyrus in the rat hippocampus immediately after SAH is accompanied by nNOS phosphorylation at Ser^{1412}. This signaling pathway might be activated by the immediate increase in ICP after the onset of SAH. The phosphorylation of nNOS at Ser^{1412} in the dentate gyrus might be the cause of cognitive deficits after SAH. Further studies using nNOS knockout mice should be performed to clarify the role of nNOS phosphorylation at Ser^{1412} and provide clues regarding potential therapeutic interventions for cognitive or memory disturbances after SAH.

Conflicts of interest

None.

Funding

This work was partially supported by Japanese Grants-in-Aid for Scientific Research (C), Grant Numbers 26462174 (K.O.) and 15K19961 (Y.A.), and a grant from the General Insurance Association of Japan (K.O.).

Acknowledgments

We thank Masahiro Kokubo for providing technical assistance.

References

[1] N.F. Kassell, T. Sasaki, A.R. Colohan, G. Nazar, Cerebral vasospasm following aneurysmal subarachnoid hemorrhage, Stroke 16 (1985) 562–572.
[2] R.L. Macdonald, R.T. Higashida, E. Keller, S.A. Mayer, A. Molyneux, A. Raabe, P. Vajkoczy, I. Wanke, D. Bach, A. Frey, et al., Clazosentan, an endothelin receptor antagonist, in patients with aneurysmal subarachnoid haemorrhage undergoing surgical clipping: a randomised, double-blind, placebo-controlled phase 3 trial (CONSCIOUS-2), Lancet Neurol. 10 (2011) 618–625.
[3] J. Cahill, J.W. Calvert, J.H. Zhang, Mechanisms of early brain injury after subarachnoid hemorrhage, J. Cereb. Blood Flow. Metab. 26 (2006) 1341–1353.
[4] M.L. Hackett, C.S. Anderson, Health outcomes 1 year after subarachnoid hemorrhage: an international population-based study. The australian cooperative Research on subarachnoid hemorrhage study group, Neurology 55 (2000) 658–662.
[5] G.K. Wong, S.W. Lam, K. Ngai, A. Wong, D. Siu, W.S. Poon, V. Mok, Cognitive Dysfunction after Aneurysmal Subarachnoid Hemorrhage I. Cognitive domain deficits in patients with aneurysmal subarachnoid haemorrhage at 1 year, J. Neurol. Neurosurg. Psychiatry 84 (2013) 1054–1058.
[6] R.J. Lichtenwalner, J.M. Parent, Adult neurogenesis and the ischemic forebrain, J. Cereb. Blood Flow. Metab. 26 (2006) 1–20.
[7] Z. Liu, Y. Fan, S.J. Won, M. Neumann, D. Hu, L. Zhou, P.R. Weinstein, J. Liu, Chronic treatment with minocycline preserves adult new neurons and reduces functional impairment after focal cerebral ischemia, Stroke 38 (2007) 146–152.
[8] M.J. Eliasson, Z. Huang, R.J. Ferrante, M. Sasamata, M.E. Molliver, S.H. Snyder, M.A. Moskowitz, Neuronal nitric oxide synthase activation and peroxynitrite formation in ischemic stroke linked to neural damage, J. Neurosci. 19 (1999) 5910–5918.
[9] Z. Huang, P.L. Huang, N. Panahian, T. Dalkara, M.C. Fishman, M.A. Moskowitz, Effects of cerebral ischemia in mice deficient in neuronal nitric oxide synthase, Science 265 (1994) 1883–1885.
[10] K. Osuka, Y. Watanabe, N. Usuda, K. Atsuzawa, M. Takayasu, Phosphorylation of neuronal nitric oxide synthase at Ser1412 in the dentate gyrus of rat brain after transient forebrain ischemia, Neurochem. Int. 63 (2013) 269–274.
[11] M.K. Richards, M.A. Marletta, Characterization of neuronal nitric oxide synthase and a C415H mutant, purified from a baculovirus overexpression system, Biochemistry 33 (1994) 14723–14732.
[12] T. Song, N. Hatano, K. Sugimoto, M. Horii, F. Yamaguchi, M. Tokuda, Y. Miyamoto, T. Kambe, Y. Watanabe, Nitric oxide prevents phosphorylation of neuronal nitric oxide synthase at Serine1412 by inhibiting the Akt/PKB and CaM-K II signaling pathways, Int. J. Mol. Med. 30 (2012) 15–20.
[13] J.B. Bederson, I.M. Germano, L. Guarino, Cortical blood flow and cerebral perfusion pressure in a new noncraniotomy model of subarachnoid hemorrhage in the rat, Stroke 26 (1995) 1086–1091 discussion 91–92.
[14] A. Jackowski, A. Crockard, G. Burnstock, R.R. Russell, F. Kristek, The time course of intracranial pathophysiological changes following experimental subarachnoid haemorrhage in the rat, J. Cereb. Blood Flow. Metab. 10 (1990) 835–849.
[15] R.A. Solomon, J.L. Antunes, R.Y. Chen, L. Bland, S. Chien, Decrease in cerebral blood flow in rats after experimental subarachnoid hemorrhage: a new animal model, Stroke 16 (1985) 58–64.
[16] J.Y. Lee, O. Sagher, R. Keep, Y. Hua, G. Xi, Comparison of experimental rat models of early brain injury after subarachnoid hemorrhage, Neurosurgery 65 (2009) 331–343 discussion 43.
[17] E. Grote, W. Hassler, The critical first minutes after subarachnoid hemorrhage, Neurosurgery 22 (1988) 654–661.
[18] T. Zoerle, A. Lombardo, A. Colombo, L. Longhi, E.R. Zanier, P. Rampini, N. Stocchetti, Intracranial pressure after subarachnoid hemorrhage, Crit. Care Med. 43 (2015) 168–176.
[19] R. Nau, S. Haase, S. Bunkowski, W. Bruck, Neuronal apoptosis in the dentate gyrus in humans with subarachnoid hemorrhage and cerebral hypoxia, Brain Pathol. 12 (2002) 329–336.
[20] S. Marbacher, V. Neuschmelting, L. Andereggen, H.R. Widmer, M. von Gunten, J. Takala, S.M. Jakob, J. Fandino, Early brain injury linearly correlates with reduction in cerebral perfusion pressure during the hyperacute phase of subarachnoid hemorrhage, Intensive Care Med. Exp. 2 (2014) 30.
[21] J.A. Frontera, W. Ahmed, V. Zach, M. Jovine, L. Tanenbaum, F. Sehba, A. Patel, J.B. Bederson, E. Gordon, Acute ischaemia after subarachnoid haemorrhage, relationship with early brain injury and impact on outcome: a prospective quantitative MRI study, J. Neurol. Neurosurg. Psychiatry 86 (2015) 71–78.
[22] K. Sato, H. Shimizu, M. Fujimura, T. Inoue, Y. Matsumoto, T. Tominaga, Acute-stage diffusion-weighted magnetic resonance imaging for predicting outcome of poor-grade aneurysmal subarachnoid hemorrhage, J. Cereb. Blood Flow. Metab. 30 (2010) 1110–1120.
[23] P.G. Matz, M. Fujimura, P.H. Chan, Subarachnoid hemolysate produces DNA fragmentation in a pattern similar to apoptosis in mouse brain, Brain Res. 858 (2000) 312–319.
[24] T. Abel, P.V. Nguyen, M. Barad, T.A. Deuel, E.R. Kandel, R. Bourtchouladze, Genetic demonstration of a role for PKA in the late phase of LTP and in hippocampus-based long-term memory, Cell. 88 (1997) 615–626.
[25] J. Aronowski, J.C. Grotta, M.N. Waxham, Ischemia-induced translocation of Ca2+/calmodulin-dependent protein kinase II: potential role in neuronal damage, J. Neurochem. 58 (1992) 1743–1753.
[26] H. Yamamoto, K. Fukunaga, K. Lee, T.R. Soderling, Ischemia-induced loss of brain calcium/calmodulin-dependent protein kinase II, J. Neurochem. 58 (1992) 1110–1117.
[27] K. Tanaka, Y. Fukuuchi, H. Nozaki, E. Nagata, T. Kondo, T. Dembo, Acute ischemic vulnerability of PKA in the dendritic subfields of the hippocampus CA1, Neuroreport 8 (1997) 2423–2428.
[28] D.S. Bredt, C.D. Ferris, S.H. Snyder, Nitric oxide synthase regulatory sites. Phosphorylation by cyclic AMP-dependent protein kinase, protein kinase C, and calcium/calmodulin protein kinase; identification of flavin and calmodulin binding sites, J. Biol. Chem. 267 (1992) 10976–10981.
[29] B. Brune, E.G. Lapetina, Phosphorylation of nitric oxide synthase by protein kinase A, Biochem. Biophys. Res. Commun. 181 (1991) 921–926.
[30] J.L. Dinerman, J.P. Steiner, T.M. Dawson, V. Dawson, S.H. Snyder, Cyclic nucleotide dependent phosphorylation of neuronal nitric oxide synthase inhibits catalytic activity, Neuropharmacology 33 (1994) 1245–1251.
[31] Y. Hayashi, M. Nishio, Y. Naito, H. Yokokura, Y. Nimura, H. Hidaka, Y. Watanabe, Regulation of neuronal nitric-oxide synthase by calmodulin kinases, J. Biol. Chem. 274 (1999) 20597–20602.
[32] K. Komeima, Y. Hayashi, Y. Naito, Y. Watanabe, Inhibition of neuronal nitric-oxide synthase by calcium/calmodulin-dependent protein kinase IIalpha through Ser847 phosphorylation in NG108-15 neuronal cells, J. Biol. Chem. 275 (2000) 28139–28143.
[33] T. Song, N. Hatano, M. Horii, H. Tokumitsu, F. Yamaguchi, M. Tokuda, Y. Watanabe, Calcium/calmodulin-dependent protein kinase I inhibits neuronal nitric-oxide synthase activity through serine 741 phosphorylation, FEBS Lett. 570 (2004) 133–137.
[34] K.J. Hurt, S.F. Sezen, G.F. Lagoda, B. Musicki, G.A. Rameau, S.H. Snyder, A.L. Burnett, Cyclic AMP-dependent phosphorylation of neuronal nitric oxide synthase mediates penile erection, Proc. Natl. Acad. Sci. U. S. A 109 (2012) 16624–16629.
[35] M. Khan, T.S. Dhammu, F. Matsuda, A.K. Singh, I. Singh, Blocking a vicious cycle nNOS/peroxynitrite/AMPK by S-nitrosoglutathione: implication for stroke therapy, BMC Neurosci. 16 (2015) 42.
[36] R. Kar, D.L. Kellogg 3rd, L.J. Roman, Oxidative stress induces phosphorylation of neuronal NOS in cardiomyocytes through AMP-activated protein kinase (AMPK), Biochem. Biophys. Res. Commun. 459 (2015) 393–397.
[37] L. Sanchez-Ruiloba, C. Aicart-Ramos, L. Garcia-Guerra, J. Pose-Utrilla, I. Rodriguez-Crespo, T. Iglesias, Protein kinase D interacts with neuronal nitric oxide synthase

and phosphorylates the activatory residue serine 1412, PLoS One 9 (2014) e95191.
[38] P.S. Eriksson, E. Perfilieva, T. Bjork-Eriksson, A.M. Alborn, C. Nordborg, D.A. Peterson, F.H. Gage, Neurogenesis in the adult human hippocampus, Nat. Med. 4 (1998) 1313–1317.
[39] D.R. Kornack, P. Rakic, Continuation of neurogenesis in the hippocampus of the adult macaque monkey, Proc. Natl. Acad. Sci. U. S. A 96 (1999) 5768–5773.
[40] M. Adachi, M. Abe, T. Sasaki, H. Kato, J. Kasahara, T. Araki, Role of inducible or neuronal nitric oxide synthase in neurogenesis of the dentate gyrus in aged mice, Metab. Brain Dis. 25 (2010) 419–424.
[41] M.A. Packer, Y. Stasiv, A. Benraiss, E. Chmielnicki, A. Grinberg, H. Westphal, S.A. Goldman, G. Enikolopov, Nitric oxide negatively regulates mammalian adult neurogenesis, Proc. Natl. Acad. Sci. U. S. A 100 (2003) 9566–9571.
[42] D.Y. Zhu, S.H. Liu, H.S. Sun, Y.M. Lu, Expression of inducible nitric oxide synthase after focal cerebral ischemia stimulates neurogenesis in the adult rodent dentate gyrus, J. Neurosci. 23 (2003) 223–229.
[43] L. Corsani, E. Bizzoco, F. Pedata, M. Gianfriddo, M.S. Faussone-Pellegrini, M.G. Vannucchi, Inducible nitric oxide synthase appears and is co-expressed with the neuronal isoform in interneurons of the rat hippocampus after transient ischemia induced by middle cerebral artery occlusion, Exp. Neurol. 211 (2008) 433–440.
[44] C. Park, Y. Sohn, K.S. Shin, J. Kim, H. Ahn, Y. Huh, The chronic inhibition of nitric oxide synthase enhances cell proliferation in the adult rat hippocampus, Neurosci. Lett. 339 (2003) 9–12.
[45] Y. Sun, K. Jin, J.T. Childs, L. Xie, X.O. Mao, D.A. Greenberg, Neuronal nitric oxide synthase and ischemia-induced neurogenesis, J. Cereb. Blood Flow. Metab. 25 (2005) 485–492.
[46] M. Mino, H. Kamii, M. Fujimura, T. Kondo, S. Takasawa, H. Okamoto, T. Yoshimoto, Temporal changes of neurogenesis in the mouse hippocampus after experimental subarachnoid hemorrhage, Neurol. Res. 25 (2003) 839–845.
[47] K. Makino, K. Osuka, Y. Watanabe, N. Usuda, M. Hara, M. Aoyama, M. Takayasu, T. Wakabayashi, Increased ICP promotes CaMKII-mediated phosphorylation of neuronal NOS at Ser^{847} in the hippocampus immediately after subarachnoid hemorrhage, Brain Res. 1616 (2015) 19–25.
[48] J.L. Warner-Schmidt, R.S. Duman, Hippocampal neurogenesis: opposing effects of stress and antidepressant treatment, Hippocampus 16 (2006) 239–249.
[49] L. Santarelli, M. Saxe, C. Gross, A. Surget, F. Battaglia, S. Dulawa, N. Weisstaub, J. Lee, R. Duman, O. Arancio, et al., Requirement of hippocampal neurogenesis for the behavioral effects of antidepressants, Science 301 (2003) 805–809.
[50] T.D. Perera, J.D. Coplan, S.H. Lisanby, C.M. Lipira, M. Arif, C. Carpio, G. Spitzer, L. Santarelli, B. Scharf, R. Hen, et al., Antidepressant-induced neurogenesis in the hippocampus of adult nonhuman primates, J. Neurosci. 27 (2007) 4894–4901.
[51] Q.G. Zhou, Y. Hu, Y. Hua, M. Hu, C.X. Luo, X. Han, X.J. Zhu, B. Wang, J.S. Xu, D.Y. Zhu, Neuronal nitric oxide synthase contributes to chronic stress-induced depression by suppressing hippocampal neurogenesis, J. Neurochem. 103 (2007) 1843–1854.
[52] D. Berron, H. Schutze, A. Maass, A. Cardenas-Blanco, H.J. Kuijf, D. Kumaran, E. Duzel, Strong evidence for pattern separation in human dentate gyrus, J. Neurosci. 36 (2016) 7569–7579.
[53] R. Coras, E. Pauli, J. Li, M. Schwarz, K. Rossler, M. Buchfelder, H. Hamer, H. Stefan, I. Blumcke, Differential influence of hippocampal subfields to memory formation: insights from patients with temporal lobe epilepsy, Brain 137 (2014) 1945–1957.